Published in final edited form as:
Traffic. 2012 January ; 13(1): 82–93. doi:10.1111/j.1600-0854.2011.01294.x.

MICAL-L1 is a tubular endosomal membrane hub that connects Rab35 and Arf6 with Rab8a

Juliati Rahajeng, **Sai Srinivas Panapakkam Giridharan**, **Bishuang Cai**, **Naava Naslavsky***, and **Steve Caplan***
Department of Biochemistry and Molecular Biology and Eppley Cancer Center, University of Nebraska Medical Center, Omaha, Nebraska 68198-5870, USA.

Abstract

Endocytosis is a conserved process across species in which cell surface receptors and lipids are internalized from the plasma membrane. Once internalized, receptors can either be degraded or recycled back to the plasma membrane. A variety of small GTP-binding proteins regulate receptor recycling. Despite our familiarity with many of the key regulatory proteins involved in this process, our understanding of the mode by which these proteins cooperate and the sequential manner in which they function remains limited. In this study, we identify two GTP-binding proteins as interaction partners of the endocytic regulatory protein MICAL-L1. First, we demonstrate that Rab35 is a MICAL-L1 binding partner *in vivo*. Over-expression of active Rab35 impairs the recruitment of MICAL-L1 to tubular recycling endosomes, whereas Rab35 depletion promotes enhanced MICAL-L1 localization to these structures. Moreover, we demonstrate that Arf6 forms a complex with MICAL-L1 and plays a role in its recruitment to tubular endosomes. Overall, our data suggest a model in which Rab35 is a critical upstream regulator of MICAL-L1 and Arf6, while both MICAL-L1 and Arf6 regulate Rab8a function.

Keywords

MICAL-L1; Rab35; Arf6; Rab8a; effector; membrane tubules; recycling

INTRODUCTION

Endocytosis is a highly conserved process across species in which nutrients, and lipids are internalized into the cells. Upon endocytosis, newly internalized vesicles are directed to early endosomes (EE). While some receptors are sorted for lysosomal degradation, other receptors are recycled back to the plasma membrane, either in a direct pathway from EE (fast recycling) or indirectly through the endocytic recycling compartment (ERC) (reviewed in (1, 2)).

Many proteins regulate these trafficking pathways, with the Ras-like small GTP-binding proteins (Rab-GTP-binding proteins) playing a central role. The Rab-GTP-binding proteins are molecular switches that can either bind GTP when in an activated state and associate with membranes, or they are inactive, GDP-bound, and mostly localized to the cytoplasm (reviewed in (3)). The guanine nucleotide exchange factors (GEFs) of Rab proteins catalyze the exchange of GDP with GTP. Upon binding to GTP, Rab proteins recruit their molecular effectors, which are proteins that interact specifically with GTP-bound Rabs and carry out

*Address correspondence to: Steve Caplan scaplan@unmc.edu and Naava Naslavsky nnaslavsky@unmc.edu Tel: 402-559-7556 FAX: 402-559-6650.

select effector functions. Hydrolysis activity by a family of proteins known as Rab GTPase activating proteins (GAPs) facilitates conversion of Rab-GTP to Rab-GDP, and the Rab is generally released from membranes to the cytoplasm (reviewed in (3)). Particularly well studied are Rab5, which regulates trafficking of newly internalized receptors to EE, and Rab4, which is involved in both the fast and slow recycling pathways of the transferrin receptor ((4-7)).

Although many Rab proteins and the molecular mechanisms by which they control different trafficking pathways have been very well characterized, others are not as well understood. One Rab that has recently been an intense focus of study is Rab35, a member of the Rab protein family that regulates fast recycling of receptors such as major histocompatibility class I (MHC I) (8). Moreover, Rab35 is required for recycling of KCa2.3 Ca^{2+}-activated K^+ channels (9). Rab35, which is localized both to endosomes and the plasma membrane (10), is also required for endosomal secretion during immunological synapse formation and stabilization and successful abscission of the cytokinesis bridge (10, 11). In addition, Rab35 is linked to actin dynamics during neurite outgrowth and to actin bundling during bristle formation in *D. melanogaster* (12, 13). Recently, it was demonstrated that Rab35 and its novel GAP, Skywalker, regulate endosomal trafficking of synaptic vesicles at *Drosophila* neuromuscular junctions (14).

Allaire *et al*. showed that Rab35 is activated by connecdenn (8), a component of clathrin-coated vesicles that can bind to lipids or membranes through its **D**ifferentially **E**xpressed in **N**eoplastic versus **N**ormal cells (DENN) domain. The DENN domain of connecdenn binds Rab35 and functions as a GEF for this GTPase (8). Upon its activation, Rab35 presumably recruits molecular effectors to membranes. One recently described molecular effector for Rab35 is fascin, which facilitates actin bundling (12, 13). However, the identification of additional effectors and the mode by which Rab35 interacts with them to control receptor transport remains unknown.

Through a large yeast two hybrid screen, it has been shown that a constitutively active mutant of Rab35, Rab35 Q67L, can interact with two members of the Molecule Interacting with CasL (MICAL) protein family: MICAL1 and MICAL-like protein 1 (MICAL-L1) (15). We recently reported that MICAL-L1 regulates endocytic transport by its interaction with EHD1 to regulate recycling of receptors through the first of its two asparagine-prolinephenylalanine (NPF) tripeptide motifs (16, 17). In HeLa cells, MICAL-L1 localizes to tubular endosomes through its coiled-coil (CC) region and recruits EHD1 and Rab8a to these tubular recycling endosomes (17). In addition, we previously demonstrated that EHD1 is also associated with tubular membranes that contain Arf6, a key regulator of the clatrhin-independent pathway (18). Recent studies suggest that Arf6 activity is controlled by Rab35 via centaurin β2/**A**rf-GAP with **C**oiled-coil, **A**NK repeat and **P**H domain containing protein **2** (ACAP2) (19). Moreover, it has been demonstrated that one mode by which Arf6 regulates the association with EHD1 is through the activation of phosphatidylinositol 4-phosphate 5-kinase (20).

Here we show that MICAL-L1 is a novel interaction partner for Rab35. Over-expression of either wild-type Rab35 or Rab35 Q67L led to the dissociation of MICAL-L1, and subsequently Rab8a from tubular endosomes. In agreement with these findings, knock-down of Rab35 caused increased association of MICAL-L1 with tubular membranes. Our yeast two-hybrid assays suggest that the CC region of MICAL-L1 is responsible for its interaction with wild-type Rab35 or Rab35 Q67L, whereas no binding occurs with dominant-negative GDP-locked Rab 35 (Rab35 S22N). On the other hand, over-expression of either wild-type Rab10 or dominant-active Rab10 (Rab10 Q67L) did not alter MICAL-L1 localization to tubular endosomes, and Rab10-depletion similarly had little effect on MICAL-L1

localization. Moreover, we demonstrated that MICAL-L1 coimmunoprecipitates with Arf6. We also demonstrated that over-expression of Arf6 Q67L caused accumulation of Rab8a into phosphatidylinositol 4,5-bisphosphate (PIP_2)-enriched vacuoles, suggesting that Arf6 acts upstream of Rab8a. Our data provide evidence suggesting that MICAL-L1 interacts with and functions downstream of Rab35 and serves as a hub to connect the functions of Rab35, Arf6 and Rab8.

RESULTS

Rab35 expression impairs the localization of MICAL-L1 to tubular endosomes

To determine if MICAL-L1 is an effector of Rab35, we transfected HeLa cells with either wild-type Myc-Rab35, Myc-Rab35 Q67L or Myc-Rab35 S22N and monitored the localization of MICAL-L1 (Fig. 1A-F and quantified in G). Over-expression of either wild-type myc-Rab35 or myc-Rab35 Q67L induced a lack of association of MICAL-L1 with membrane tubules, whereas over-expression of Myc-Rab35 S22N did not significantly alter the level of MICAL-L1 localized to tubular endosomes (Fig. 1A-F and quantified in G).

A key question is whether the activated Rab35 removes/prevents association of MICALL1 with tubular membranes, or whether active Rab35 actually destroys or prevents biogenesis of these tubular structures. We have previously shown that EHD1 partially overlaps with GFP fused to the double palmitoylated and farnesylated carboxy-terminal tail of H-Ras (GFPH-Ras) on tubular membranes ((20) and see Fig 1H and I), and that this protein can be used as a general marker for tubular endosomes containing EHD1 and MICAL-L1. To determine whether activated Rab35 abolishes the GFP-H-Ras tubular membranes, we transfected cells with both GFP-H-Ras and Myc-Rab35 Q67L, and then triple stained to follow the localization of MICALL1, GFP-H-Ras and Myc-Rab35 Q67L (Fig 1J-L). As demonstrated, cells over-expressing Myc-Rab35 Q67L (Fig. 1L) were again almost devoid of any MICAL-L1 on tubular membranes (Fig. 1J). However, tubular membranes containing GFP-H-Ras were clearly still evident (Fig. 1K) suggesting that active Rab35 does not affect tubule biogenesis, but rather controls the association of MICAL-L1 with these structures.

Rab35-depletion increases the localization of MICAL-L1 to tubular endosomes

Since over-expression of Rab35 reduces the level of MICAL-L1 localized to tubular endosomes, we hypothesized that depletion of Rab35 might lead to enhanced MICAL-L1 on these structures. To address this, we utilized Rab35-siRNA oligonucleotides to knock-down Rab35 expression. Since detection of protein levels with antibodies to endogenous Rab35 is not feasible in the HeLa cells used in this study, to validate siRNA efficacy we used two methods: (1) over-expression of wild-type Myc-tagged Rab35 in HeLa cells treated with either mock- or Rab35-siRNA oligonucleotides, and (2) real-time PCR. The latter method demonstrated significant reduction of endogenous Rab35 mRNA in cells treated with Rab35-siRNA oligonucleotides compared to the mock-treated cells (Fig. 2A). We also showed that there is a significant reduction in the protein expression levels of Myc-Rab35 in cells treated with Rab35-siRNA oligonucleotides compared to the mock-treated cells. (Fig. 2B). In agreement with the data shown in Fig. 1, we observed increased MICAL-L1 localization to tubular endosomes upon depletion of Rab35 (Fig. 2C and D; quantified in E). Knock-down of Rab35 also led to rapid accumulation of transferrin at the ERC after 5 minutes of uptake as shown in Supplemental Fig.1 A and B. However, depletion of Rab35 did not affect the rate of transferrin recycling (Supplemental Fig. 1) or the rate of β1 integrin receptor recycling (Supplemental Fig. 2), consistent with the study of Allaire *et al.* (8). On the other hand, siRNA-based depletion of endogenous in Jurkat T cells (Supplemental Fig. 3A) caused enhanced levels of CD3 on the plasma membrane, suggesting a role for Rab35 and in T cell receptor recycling (Supplemental Fig. 3B).

Rab10 expression and depletion do not control MICAL-L1 localization to tubular endosomes

Fukuda and co-workers showed that MICAL-L1 can bind to multiple Rab proteins, including Rab35 and Rab10, when tested by yeast two-hybrid assays (15). Since Rab10 has been implicated in the regulation of endocytic trafficking (21-23), we next assessed whether MICAL-L1 was similarly affected by the over-expression of Rab10. As shown in Fig. 3, over-expression of wild-type HA-Rab10, HA-Rab10 Q67L or HA-Rab10 T23N in HeLa cells did not alter the localization of MICAL-L1. Moreover, siRNA-based depletion of Rab10 (Supplemental Fig. 4) had no visible effect on MICAL-L1 localization (Fig. 3, compare J and K). While these data do not rule a potential functional interaction between Rab10 and MICAL-L1, they indicate that active Rab35 specifically reduces MICAL-L1 localization to tubular endosomes.

Rab35 co-immunoprecipitates with MICAL-L1 and interacts with the latter's coiled-coil region

We next addressed the ability of Rab35 and MICAL-L1 to interact in mammalian cells. When HeLa cells were transfected with HAMICAL-L1 along with either wild-type Myc-Rab35 or Myc-Vps45 (negative control) and immunoprecipitated with anti-HA antibody, we were able to co-immunoprecipitate Myc-Rab35 but not Myc-Vps45 (Fig. 4A). Since the CC region of the MICAL-L1 paralog, MICAL-L2, interacts with Rab8 and Rab13, we hypothesized that the CC region of MICAL-L1 (Fig. 4B) might interact with Rab35. Indeed, the CC region of MICAL-L1 is sufficient for an interaction with the wild-type and dominant-active mutants of Rab35 (and Rab10), but not with the dominant-negative mutants of Rab35 and Rab10 (Fig. 4C).

We have previously shown that MICAL-L1 recruits Rab8a to tubular endosomes (17). An important question that arises is whether the dominant-active Rab35 affects Rab8a indirectly by its impact on MICAL-L1 localization. As demonstrated, over-expression of GFP-MICALL1 causes recruitment of Rab8a to membrane tubules (Fig. 4D-I). However, upon over-expression of Myc-Rab35 Q67L along with GFPMICAL-L1, Rab8a was absent from the tubular endosomes (Fig. 4G-I). This suggests that Rab35 regulates Rab8a tubular localization through its interaction with MICAL-L1, consistent with our earlier findings that MICAL-L1 recruits Rab8a to membranes (17).

Arf6 expression and activation causes redistribution of Rab8a

Since Arf6 activation is regulated by Rab35 via the GTPase activating protein ACAP2 (19), we next asked whether Rab8a localization to tubular membranes is also regulated by Arf6. As demonstrated, Cherry-Rab8a localized to the same tubular endosomes containing wild-type FLAG-Arf6 (Fig. 5). However, over-expression of the dominant-active Arf6 (FLAG-Arf6 Q67L) in HeLa cells led to accumulation of Cherry-Rab8a in the Arf6/PIP_2-containing vacuoles. Moreover, over-expression of FLAG-EFA6, which activates Arf6, also led to dissociation of Cherry-Rab8a from tubular endosomes (Supplemental Fig. 5). On the other hand, over-expression of dominant-negative Arf6 (FLAG-Arf6 T27N) caused recruitment of Cherry-Rab8a to membrane tubules (Fig. 5H-J). These results support the notion that Arf6 determines the morphology of the membrane structures to which Rab8a localizes, consistent with the findings of Hattula *et al*. (24).

Arf6 interacts with MICAL-L1 and its depletion causes the loss of MICAL-L1 on tubular endosomes

Given that Arf6 directly affects recruitment of Rab8a to tubular endosomes, we rationalized that the effect of Arf6 on Rab8a might be mediated, at least in part, through MICAL-L1. As

demonstrated in Fig. 6, upon depletion of Arf6 the level of MICAL-L1 that localized to tubular membranes was significantly decreased (Fig. 6, compare B to A; see insets). Because there are no Arf6 antibodies described in the literature capable of detecting endogenous Arf6 levels, we demonstrated efficacy of Arf6-depletion by showing that high levels of transfected FLAG-tagged Arf6 could be dramatically reduced with Arf6-siRNA (Fig. 6C). However, upon transfection of a siRNA-resistant form of Arf6 back into Arf6-depleted cells (see white borders in 6E-G), MICAL-L1 was again found primarily associated with membrane tubules. Quantification and statistical analysis of several hundred cells from three independent experiments showed a significant difference in the levels of tubule-localized MICAL-L1 between Mock and Arf6-depleted cells (Fig. 6D; p=0.04). Transfection of an siRNA-resistant wild-type (WT) Arf6 into the depleted cells led to a slight but consistent increase in the percentage of cells with MICAL-L1 localized to tubular membranes. However, the calculated statistical significance of this increase is not as clear (p=0.18). Overall, these data suggest that Arf6 can regulate Rab8a localization either directly or via MICAL-L1.

We have identified MICAL-L1 as a central hub connecting to Rab35 both functionally and through a physical interaction. In Fig. 6, we have also demonstrated that Arf6 functionally regulates MICAL-L1 localization. These findings raised the question as to whether MICAL-L1 and Arf6 physically interact.

To determine whether Arf6 and MICALL1 interact with one another, we transfected HeLa cells with wild-type HA-Arf6 and either full-length GFP-MICAL-L1, or a truncated GFPMICAL-L1 mutant lacking its membrane-binding coiled-coil region (GFP-MICAL-L1 ΔCC). As demonstrated, immunoblot analysis of transfected cells showed similar levels of full-length GFP-MICAL-L1 and GFP-MICAL-L1 ΔCC (Fig. 6H; upper panel. Note that the truncated MICAL-L1 is reduced in apparent molecular weight). Slightly higher levels of HA-Arf6 were detected in the cells transfected with the truncated MICAL-L1 mutant. Upon co-immunoprecipitation to examine whether MICAL-L1 is found in a complex with ARF6, we demonstrated that Arf6 is capable of immunoprecipitating GFP-MICAL-L1, but not GFP-MICAL-L1 ΔCC (Fig. 6H; lower panel). These data are the first to demonstrate an interaction between Arf6 and MICAL-L1, and support a key role MICAL-L1 as a central hub regulated both by Rab35 and Arf6.

DISCUSSION

Upon internalization, cell surface receptors can undergo multiple fates that include degradation or recycling back to the plasma membrane. The various intracellular trafficking pathways of receptors are regulated by a wide variety of small GTP-binding proteins such as the Arf, Rho and Rab families. More than 60 members of mammalian Rab proteins have been identified (25), whereas the Arf protein family consists of 6 human members (26). The Rho protein family controls actin and microtubules, has 22 mammalian members and is also involved in the regulation of intracellular trafficking (27).

Several members of the Rab and Arf protein families regulate receptor recycling. For example, Rab11 controls recycling of transferrin receptor (28) and β1 integrin receptors (29) from the ERC back to the plasma membrane. Rab35 controls the recycling of various proteins including transferrin receptors (10), MHC I molecules (8), and Ca2+-activated K+ (KCa2.3) channels in *C. elegans* (9). It has also been implicated in exosome secretion in neuronal cells (30). Recently, Rab35 has also been implicated in control of the actin cytoskeleton and cytokinesis (12, 13, 31, 32) and the control of T cell antigen receptor localization to the immunologic synapse (11). On the other hand, Rab8a regulates both secretion and receptor recycling (33-36).

Of the Arf proteins, only Arf6 regulates recycling (26). Arf6 cooperates with Rab11 to regulate recycling from the ERC back to the plasma membrane through interactions with the effector proteins Rab11-FIP3 and Rab11-FIP4 (37). Another example of cooperation between Rab and Arf proteins is that Arf6 co-localizes with and is functionally linked to Rab8a (24). Arf6 activity is also regulated by Rab35 through its interaction with ACAP2 (19). However, the spatio-temporal relationship between the various regulatory proteins that underlies the control of endocytic recycling is poorly understood.

A prime candidate as a “hub” to connect the key small GTP-binding proteins involved in the recycling process is MICAL-L1. Originally identified as an interaction partner for EHD1, MICAL-L1 regulates membrane recycling and localizes to tubular endosomes through its C-terminal coiled-coil region (17). In addition, over-expression of MICAL-L1 in HeLa cells led to recruitment of Rab8a to tubular endosomes, whereas its depletion led to loss of both EHD1 and Rab8a from these structures (17).

Since MICAL-L1 is required for Rab8a localization to tubular endosomes and not *vice versa*, MICAL-L1 does not fit the typical description of a classical Rab8a effector. We reasoned, therefore, that it might physically and functionally interact with other Rab proteins. Indeed, a MICAL-L1 is able to bind to several Rabs, including Rab35, at least in a yeast two-hybrid system (19). Because of Rab35's role in selectively controlling cargo exit from the EE (8), and its regulation of Arf6 (19), we rationalized that MICAL-L1 might serve as a key protein to link GTP-binding proteins from the Arf and Rab families.

In this study, we showed that MICAL-L1 serves as a “scaffold” or functional hub that links several small GTP-binding proteins in regulating receptor trafficking through the ERC (Fig. 6I). Knock-down of Rab35 increases the level of MICAL-L1 localized to tubular membranes and over-expression of either wild-type Rab35 or the active Rab35 Q67L form has the opposite effect. On the other hand, over-expression of Rab35 led to dissociation of Rab8 a from tubular endosomes, likely as a result of its impact on MICAL-L1.

Rab35 may also regulate the localization of MICAL-L1 indirectly through activation of Arf6 (see Fig. 6I). ACAP2, which hydrolyzes Arf6-GTP, interacts with Rab35 (19). Therefore, activation of Rab35 led to inactivation of Arf6 (19). Our data showed that depletion of Arf6 decreased MICAL-L1 localization to tubular endosomes. Thus activation of Rab35 (which inactivates Arf6) reduced the localization of MICAL-L1 to tubular recycling endosomes, displacing Rab8a from these structures. However, Arf6 may directly regulate Rab8a localization, as both proteins participate in the formation of recycling tubules and cell protrusions (24).

In addition, we have demonstrated for the first time that MICAL-L1 is also found in a complex with Arf6, and that expression of Arf6 is required for the association of MICAL-L1 with tubular endosomes. These data further support our model by which Arf6 and Rab35 have antagonistic effects on the localization of MICAL-L1 (Fig. 6I).

In conclusion, we found that depletion of Rab35 led to increased localization of MICAL-L1 to tubular recycling endosomes, whereas over-expression of wild-type Rab35 or Rab35 Q67L had the opposite effect, leading to the dissociation Rab8a from these structures as well. These results suggest a novel function for MICAL-L1 downstream of Rab35. Despite its ability to interact with Rab10 through yeast two-hybrid assays, MICAL-L1 remains unaffected by expression levels of GTP-locked, GDP-locked or endogenous Rab10, since over-expression of wild-type Rab10 or Rab10 Q67L or siRNA depletion had no impact on MICAL-L1 localization. Although depletion of Rab35 did not alter the kinetics of transferrin or β1 integrin receptors trafficking, it did lead to accumulation of transferrin at the perinuclear region upon 5 minutes of transferrin uptake. However, in Jurkat T cells,

depletion of Rab35 did lead to increased levels of T cell antigen receptor (TCR) CD3 subunits detected on the plasma membrane, consistent with the study of Patino-Lopez et al., who demonstrated a role for Rab35 in localization of the TCR to the immunologic synapse (Patino-Lopez et al.). While the mechanism for this enhanced TCR surface expression remains to be identified, it is possible to speculate that the loss of Rab35 expression in these cells potentially causes enhanced TCR recycling resulting from an excess of MICAL-L1 localization to tubular recycling endosomes. However, additional studies will be necessary to address this. Finally, we demonstrated that Rab35 may indirectly affect MICAL-L1 through its regulation of Arf6, as depletion of Arf6 led to decreased MICAL-L1 localization to tubular endosomes. Overall, our data provide support for the role of MICAL-L1 as an *in vivo* interaction partner for Rab35 that acts as a "hub" to connect key small GTP-binding proteins, thus facilitating endocytic recycling.

MATERIALS AND METHODS

Recombinant DNA Constructs

Wild-type Myc-Rab35, myc-Rab35 Q67L and myc-Rab35 S22N constructs were generously provided by Dr. Peter McPherson. Wild-type FLAG-Arf6, FLAG-Arf6-Q67L, and FLAG-Arf6 T27N, wild-type HA-Arf6, HA-Arf6 Q67L, HA-Arf6 T27N and FLAG-EFA6 constructs were kindly provided by Dr. Julie Donaldson. Wild-type Cherry-Rab8a, cherry-Rab8a Q79L and cherry-Rab8a T22N were generous constructs from Dr. James Goldenring. Wild-type human 3XHARab10 in pCDNA3.1(+) vector was purchased from Missouri S&T cDNA Resource Center (Rolla, MO). 3XHA-Rab10 Q67L, 3XHA-Rab10 T22N and wild-type Arf6-siRNA resistant (si-FLAG-Arf6) constructs were generated using QuickChange Site-Directed Mutagenesis Kit (Stratagene, La Jolla, CA). Wild-type Rab10, Rab10 Q67L, Rab10 T22N, wild-type Rab35, Rab35 Q67L and Rab35 S22N were modified by generation of a stop codon prior to the last two c-terminal cysteine residues and sub-cloned into the pGBKT7 vector using restriction enzymes EcoRI and BamHI. Cloning of human HA-MICALL1, MICAL-L1 in pGADT7 vector, MICAL-L1 700-863 in pGADT7 vector and myc-Vps45 has been described previously (17, 38).

Antibodies

The following antibodies and reagent were used in this study: rabbit anti-Arf6 antibody (a generous gift from Dr. Julie Donaldson), mouse anti-MICAL-L1 (Novus Biologicals, Littleton, CO), mouse anti-human β1 integrin (AbD Serotec, Raleigh, NC), goat anti-HA immobilized agarose (Bethyl, Montgomery, TX), mouse anti-FLAG M2 (Sigma, St. Louis, MO), rabbit anti-FLAG (GeneTex, Irvine, CA), mouse anti-myc 9E10 (Covance, Berkeley, CA), mouse anti-HA (Covance), mouse anti-CD3 (BD Biosciences, San Jose, CA), rabbit anti-Rab35 (ProteinTech, Chicago, Il), HRP-conjugated goat anti-mouse Fcγ fragment specific (Jackson ImmunoResearch, West Grove, PA), 488-conjugated goat anti-mouse (Molecular Probes, Eugene, OR) and 633-conjugated and 568-conjugated human transferrin (Molecular Probes).

Immunoprecipitations and immunoblotting

For immunoprecipitation experiments, HeLa cells transfected with HA-MICAL-L1 and either wild-type myc-Rab35 or myc-Vps45, were harvested and lysed for 30 min in buffer containing 25 mM Tris, pH 7.4, 100 mM NaCl, 0.5% CHAPS (wt/vol), 1 mM $MgCl_2$ and 10 μg/mL APMSF. After removal of insoluble material by centrifugation, supernatant lysate was subjected to immunoprecipitations with goat anti-HA immobilized agarose beads for 2 h, washed three times with lysis buffer containing 0.1% CHAPS. For immunoprecipitations with MICAL-L1 and Arf6, lysis buffer included 1% Brij 98, 150 mM NaCl (Sigma Aldrich, St. Louis, MO) and GTPγS. After immunoprecipitations, proteins were eluted by boiling in

the presence of 1% SDS. Proteins were separated by 10% SDS-PAGE, transferred into nitrocellulose membrane, blocked with 5% milk in PBS, and immunoblotted with either mouse anti-HA or mouse anti-myc antibodies followed by HRP-conjugated goat anti-mouse Fcγ fragment specific antibody.

Yeast two-hybrid analysis

The yeast two hybrid assays have been described previously (39).

Gene knockdown by RNA silencing

Rab35 and Arf6 ON-TARGET*plus* SMARTpool siRNA oligonucleotides (synthesized by Dharmacon, Lafayette, CO) were transfected using Dharmafect I (Dharmacon) for 72 h as described previously (17). For Jurkat T cells, si RNA knock-down was achieved by electroporation using the Amoxa Nucleofector (Lanza, Basel, Switzerland) following the manufacturer's optimized protocol for Jurkat cells using 1×10^6 cells per point.

Immunofluorescence, transferrin and β1 integrin uptake and recycling assays

HeLa cells were grown on cover-glasses, transfected with FuGENE6 (Roche Diagnostics, Indianapolis, IN), and fixed with 4% (vol/vol) paraformaldehyde as described previously (Caplan et al., 2001). Fixed cells were incubated with primary antibodies prepared in staining solution (0.2% saponin (wt/vol) and 0.5% (wt/vol) bovine serum albumin in PBS) for 1 h at room temperature. After washes with PBS, cells were incubated with the appropriate fluorochromeconjugated secondary antibodies prepared in staining solution for 30 min at room temperature. Images were obtained using a Zeiss LSM 5 Pascal confocal microscope (Carl Zeiss, Thornwood, NY) by using a 63 X 1.4 numerical aperture objective with appropriate filters.

For transferrin uptake and recycling assays, cells were incubated in starvation media (0.5% BSA (wt/vol) in DMEM lacking serum) for 30 min at 37°C. 568-conjugated human transferrin was internalized for 5 min at 37°C. Cells were either fixed and mounted as described above or chased in complete media (DMEM with serum) for the indicated time points before fixation.

To quantify transferrin recycling by flow cytometry, HeLa cells were treated with Rab35 siRNA or mock-treated. After 72 h, the cells were serum-starved for 30 min, pulsed with 633-conjugated human transferrin and chased in complete media for the indicated time points. Following trypsinization and fixation, cells were subjected to analysis with flow cytometry.

For β1 integrin uptake and recycling assays, cells were incubated in starvation media for 1 h at 37°C. Mouse anti-human β1 integrin antibody was bound and internalized for either 30 min or 1 h at 37°C. Membrane-bound antibody was removed by acid wash for 1 min and cells were either fixed and subjected to secondary antibody immunostaining as described above or chased in complete media for 2 h. Upon chase, membrane-bound antibody was removed by acid wash and cells were fixed and visualized by immunostaining using 568-conjugated goat anti-mouse antibody. Images were obtained using a LSM 5 Pascal confocal microscope and one hundred cells from each treatment (three independent experiments) were quantified for the intensity of internalized β1 integrin using LSM5 Pascal software.

Real time PCR

Total RNA was isolated from HeLa cells that were either mock-treated or treated with Rab35 siRNA oligonucleotides using RNeasy Mini Kit (Qiagen, Valencia, CA). 2 μg of total RNA from each treatment was reverse transcribed in independent triplicates using

SuperScript III First-Strand Synthesis System for RT-PCR (Invitrogen, Carlsbad, CA). cDNA samples were diluted 1:100 and real time PCR was performed in triplicate for each primer using SYBR Green PCR Master Mix (Applied Biosystems). PCR products of approximately 200 nucleotides were amplified with primers selected using Primer Express 2.0 software program. The sequences of primers used for Rab 35 are 5' TGGCTTCACGAAATCAACCA 3' (forward primer) and 5' ACCAGCTCCGTGATGCAGTT 3' (reverse primer); the sequences of primers used for β-Actin are 5' CTTAGTTGCGTTACACCCTTTCTTG 3' (forward primer) and 5' CGGCCACATTGTGAACTTTG 3' (reverse primer). Reactions were quantified using an ABI 7500 Real Time PCR instrument and analyzed with accompanying software. Relative expression levels were determined by normalizing cycle threshold values for each Rab35 primer to the amount of β-Actin expressed ($1000/2^{(Ct\ gene-Ct\ \beta\text{-}Actin)}$). Relative fold change was calculated from normalized values.

Supplementary Material

Refer to Web version on PubMed Central for supplementary material.

Acknowledgments

We thank Dr. J. Donaldson, Dr. P. McPherson and Dr. J. Goldenring for generously providing antibodies and/or constructs. This work was supported by National Institutes of Health Grants R01GM074876 (to S. C. and N. N.) and R01GM087455 (S. C.) and National Center for Research Resources Grant P20 RR018759 (to N. N. and J. R.). This work was also supported by a grant from the Nebraska Department of Health (to N. N.)

REFERENCES

1. Grant BD, Donaldson JG. Pathways and mechanisms of endocytic recycling. Nat Rev Mol Cell Biol. 2009; 10(9):597–608. [PubMed: 19696797]
2. Maxfield FR, McGraw TE. Endocytic recycling. Nat Rev Mol Cell Biol. 2004; 5(2):121–132. [PubMed: 15040445]
3. Grosshans BL, Ortiz D, Novick P. Rabs and their effectors: achieving specificity in membrane traffic. Proc Natl Acad Sci U S A. 2006; 103(32):11821–11827. [PubMed: 16882731]
4. de Wit H, Lichtenstein Y, Kelly RB, Geuze HJ, Klumperman J, van der Sluijs P. Rab4 regulates formation of synaptic-like microvesicles from early endosomes in PC12 cells. Mol Biol Cell. 2001; 12(11):3703–3715. [PubMed: 11694600]
5. Deneka M, van der Sluijs P. 'Rab'ing up endosomal membrane transport. Nat Cell Biol. 2002; 4(2):E33–35. [PubMed: 11835054]
6. Sheff DR, Daro EA, Hull M, Mellman I. The receptor recycling pathway contains two distinct populations of early endosomes with different sorting functions. J Cell Biol. 1999; 145(1):123–139. [PubMed: 10189373]
7. van der Sluijs P, Hull M, Webster P, Male P, Goud B, Mellman I. The small GTP-binding protein rab4 controls an early sorting event on the endocytic pathway. Cell. 1992; 70(5):729–740. [PubMed: 1516131]
8. Allaire PD, Marat AL, Dall'Armi C, Di Paolo G, McPherson PS, Ritter B. The Connecdenn DENN domain: a GEF for Rab35 mediating cargo-specific exit from early endosomes. Mol Cell. 37(3): 370–382. [PubMed: 20159556]
9. Gao Y, Balut CM, Bailey MA, Patino-Lopez G, Shaw S, Devor DC. Recycling of the Ca2+-activated K+ channel, KCa2.3 is dependent upon RME-1, Rab35/EPI64C and an N-terminal domain. J Biol Chem.
10. Kouranti I, Sachse M, Arouche N, Goud B, Echard A. Rab35 regulates an endocytic recycling pathway essential for the terminal steps of cytokinesis. Curr Biol. 2006; 16(17):1719–1725. [PubMed: 16950109]

11. Patino-Lopez G, Dong X, Ben-Aissa K, Bernot KM, Itoh T, Fukuda M, Kruhlak MJ, Samelson LE, Shaw S. Rab35 and its GAP EPI64C in T cells regulate receptor recycling and immunological synapse formation. J Biol Chem. 2008; 283(26):18323–18330. [PubMed: 18450757]
12. Chevallier J, Koop C, Srivastava A, Petrie RJ, Lamarche-Vane N, Presley JF. Rab35 regulates neurite outgrowth and cell shape. FEBS Lett. 2009; 583(7):1096–1101. [PubMed: 19289122]
13. Zhang J, Fonovic M, Suyama K, Bogyo M, Scott MP. Rab35 controls actin bundling by recruiting fascin as an effector protein. Science. 2009; 325(5945):1250–1254. [PubMed: 19729655]
14. Uytterhoeven V, Kuenen S, Kasprowicz J, Miskiewicz K, Verstreken P. Loss of skywalker reveals synaptic endosomes as sorting stations for synaptic vesicle proteins. Cell. 145(1):117–132. [PubMed: 21458671]
15. Fukuda M, Kanno E, Ishibashi K, Itoh T. Large scale screening for novel rab effectors reveals unexpected broad Rab binding specificity. Mol Cell Proteomics. 2008; 7(6):1031–1042. [PubMed: 18256213]
16. Kieken F, Sharma M, Jovic M, Giridharan SS, Naslavsky N, Caplan S, Sorgen PL. Mechanism for the selective interaction of C-terminal Eps15 homology domain proteins with specific Asn-Pro-Phe-containing partners. J Biol Chem. 285(12):8687–8694. [PubMed: 20106972]
17. Sharma M, Giridharan SS, Rahajeng J, Naslavsky N, Caplan S. MICAL-L1 links EHD1 to tubular recycling endosomes and regulates receptor recycling. Mol Biol Cell. 2009; 20(24):5181–5194. [PubMed: 19864458]
18. Caplan S, Naslavsky N, Hartnell LM, Lodge R, Polishchuk RS, Donaldson JG, Bonifacino JS. A tubular EHD1-containing compartment involved in the recycling of major histocompatibility complex class I molecules to the plasma membrane. EMBO J. 2002; 21(11):2557–2567. [PubMed: 12032069]
19. Kanno E, Ishibashi K, Kobayashi H, Matsui T, Ohbayashi N, Fukuda M. Comprehensive screening for novel rab-binding proteins by GST pull-down assay using 60 different mammalian Rabs. Traffic. 11(4):491–507. [PubMed: 20070612]
20. Jovic M, Kieken F, Naslavsky N, Sorgen PL, Caplan S. Eps15 homology domain 1-associated tubules contain phosphatidylinositol-4-phosphate and phosphatidylinositol-(4,5)-bisphosphate and are required for efficient recycling. Mol Biol Cell. 2009; 20(11):2731–2743. [PubMed: 19369419]
21. Babbey CM, Ahktar N, Wang E, Chen CC, Grant BD, Dunn KW. Rab10 regulates membrane transport through early endosomes of polarized Madin-Darby canine kidney cells. Mol Biol Cell. 2006; 17(7):3156–3175. [PubMed: 16641372]
22. Larance M, Ramm G, Stockli J, van Dam EM, Winata S, Wasinger V, Simpson F, Graham M, Junutula JR, Guilhaus M, James DE. Characterization of the role of the Rab GTPase-activating protein AS160 in insulin-regulated GLUT4 trafficking. J Biol Chem. 2005; 280(45):37803–37813. [PubMed: 16154996]
23. Shi A, Chen CC, Banerjee R, Glodowski D, Audhya A, Rongo C, Grant BD. EHBP-1 functions with RAB-10 during endocytic recycling in Caenorhabditis elegans. Mol Biol Cell. 21(16):2930–2943. [PubMed: 20573983]
24. Hattula K, Furuhjelm J, Tikkanen J, Tanhuanpaa K, Laakkonen P, Peranen J. Characterization of the Rab8-specific membrane traffic route linked to protrusion formation. J Cell Sci. 2006; 119(Pt 23):4866–4877. [PubMed: 17105768]
25. Zerial M, McBride H. Rab proteins as membrane organizers. Nat Rev Mol Cell Biol. 2001; 2(2): 107–117. [PubMed: 11252952]
26. Donaldson JG, Honda A. Localization and function of Arf family GTPases. Biochem Soc Trans. 2005; 33(Pt 4):639–642. [PubMed: 16042562]
27. Heasman SJ, Ridley AJ. Mammalian Rho GTPases: new insights into their functions from in vivo studies. Nat Rev Mol Cell Biol. 2008; 9(9):690–701. [PubMed: 18719708]
28. Wilcke M, Johannes L, Galli T, Mayau V, Goud B, Salamero J. Rab11 regulates the compartmentalization of early endosomes required for efficient transport from early endosomes to the trans-golgi network. J Cell Biol. 2000; 151(6):1207–1220. [PubMed: 11121436]
29. Powelka AM, Sun J, Li J, Gao M, Shaw LM, Sonnenberg A, Hsu VW. Stimulation-dependent recycling of integrin beta1 regulated by ARF6 and Rab11. Traffic. 2004; 5(1):20–36. [PubMed: 14675422]

30. Hsu C, Morohashi Y, Yoshimura S, Manrique-Hoyos N, Jung S, Lauterbach MA, Bakhti M, Gronborg M, Mobius W, Rhee J, Barr FA, Simons M. Regulation of exosome secretion by Rab35 and its GTPase-activating proteins TBC1D10A-C. J Cell Biol. 189(2):223–232. [PubMed: 20404108]

31. Dambournet D, Machicoane M, Chesneau L, Sachse M, Rocancourt M, El Marjou A, Formstecher E, Salomon R, Goud B, Echard A. Rab35 GTPase and OCRL phosphatase remodel lipids and F-actin for successful cytokinesis. Nat Cell Biol. 13(8):981–988. [PubMed: 21706022]

32. Prekeris R. Actin regulation during abscission: unexpected roles of Rab35 and endocytic transport. Cell Res. 21(9):1283–1285. [PubMed: 21844893]

33. Henry L, Sheff DR. Rab8 regulates basolateral secretory, but not recycling, traffic at the recycling endosome. Mol Biol Cell. 2008; 19(5):2059–2068. [PubMed: 18287531]

34. Huber LA, Pimplikar S, Parton RG, Virta H, Zerial M, Simons K. Rab8, a small GTPase involved in vesicular traffic between the TGN and the basolateral plasma membrane. J Cell Biol. 1993; 123(1):35–45. [PubMed: 8408203]

35. Linder MD, Uronen RL, Holtta-Vuori M, van der Sluijs P, Peranen J, Ikonen E. Rab8-dependent Recycling Promotes Endosomal Cholesterol Removal in Normal and Sphingolipidosis Cells. Mol Biol Cell. 2006

36. Sato T, Mushiake S, Kato Y, Sato K, Sato M, Takeda N, Ozono K, Miki K, Kubo Y, Tsuji A, Harada R, Harada A. The Rab8 GTPase regulates apical protein localization in intestinal cells. Nature. 2007; 448(7151):366–369. [PubMed: 17597763]

37. Hickson GR, Matheson J, Riggs B, Maier VH, Fielding AB, Prekeris R, Sullivan W, Barr FA, Gould GW. Arfophilins are dual Arf/Rab 11 binding proteins that regulate recycling endosome distribution and are related to Drosophila nuclear fallout. Mol Biol Cell. 2003; 14(7):2908–2920. [PubMed: 12857874]

38. Rahajeng J, Caplan S, Naslavsky N. Common and distinct roles for the binding partners Rabenosyn-5 and Vps45 in the regulation of endocytic trafficking in mammalian cells. Exp Cell Res. 2009

39. Naslavsky N, Rahajeng J, Sharma M, Jovic M, Caplan S. Interactions between EHD Proteins and Rab11-FIP2: A Role for EHD3 in Early Endosomal Transport. Mol Biol Cell. 2006; 17(1):163–177. [PubMed: 16251358]

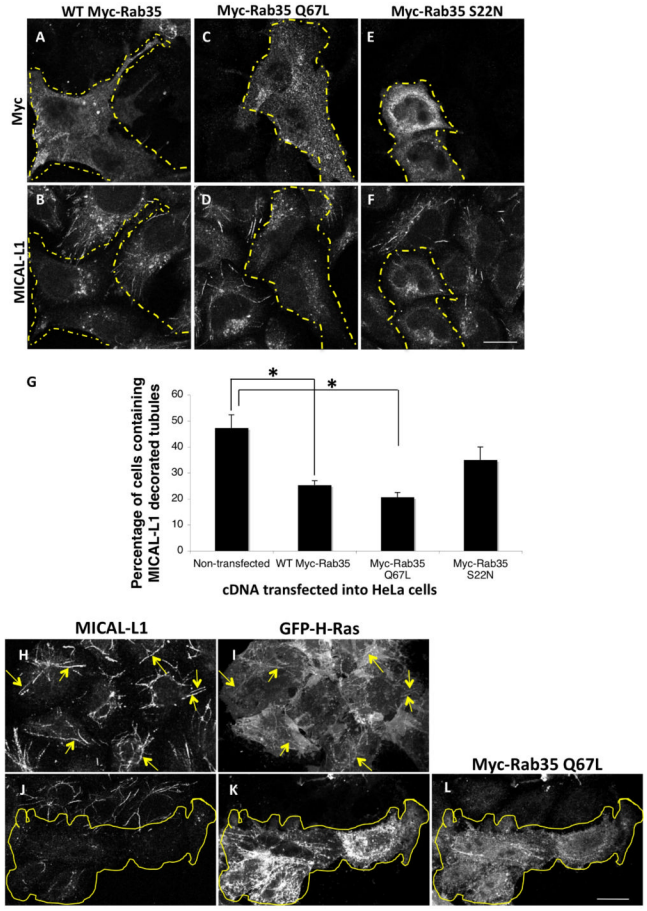

Figure 1. Rab35 expression leads to MICAL-L1 dissociation from membrane tubules

(A-F) HeLa cells were transfected with either WT Myc-Rab35 (A and B), Myc-Rab35 Q67L (C and D) or Myc-Rab35 S22N (E and F). After 24 h, cells were fixed and immunostained with anti-MICALL1 and anti-Myc antibodies. (G) Quantification of cells containing MICAL-L1 decorated tubules upon transfection with either WT Myc-Rab35, Myc-Rab35 Q67L or Myc-Rab35 S22N. One hundred cells of each treatment from three independent experiments were quantified. Error bars denote standard error. Dashed borders depict transfected cells. * p value <0.05. (H-L) HeLa cells grown on cover-slips were either transfected with GFP fused to the double palmitoylated and farnesylated carboxy-terminal tail of H-Ras (GFP-H-Ras; H and I) or both GFPH-Ras together with the activated Myc-Rab35 Q67L mutant (J-L). After 72 h, cells were fixed and permeabilized, and either immunostained with anti-MICAL-L1 antibodies (H and I), or immunostained with both anti-MICAL-L1 antibodies and anti-Myc epitope antibodies (J-L). Images were obtained in two channels (MICALL1 and GFP-H-Ras; H and I) or 3 channels (MICAL-L1, GFP-H-Ras and Myc Rab35 Q67L; J-L). Arrows in H and I denote endogenous MICAL-L1 and GFP-H-Ras partially co-localizing to the same tubular endosomes. The yellow- bordered region (J-L) depicts cells transfected with Myc-Rab35 Q67L. Note that while the MICAL-L1 in these cells is no longer associated with tubules (J), GFP-H-Ras is still clearly localized to tubular endosomes (K). Bars, 10 μm.

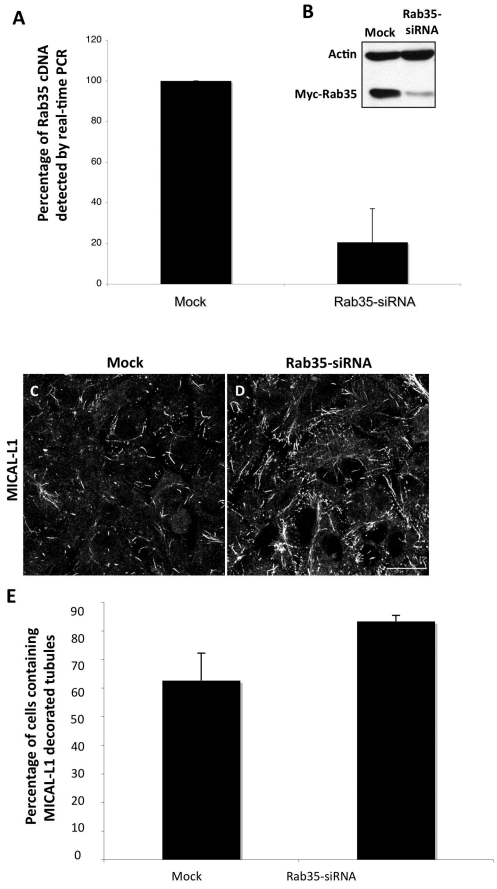

Figure 2. Rab35 depletion leads to increased MICAL-L1 localization to tubular endosomes

HeLa cells grown on 35 mm dishes or cover-slips were either mock-treated or treated with Rab35-siRNA for 72 h. (A) Cells from three independent experiments were harvested and total RNA was extracted. cDNA was reverse-transcribed from 2 μg of total RNA and subjected to real-time PCR. (B) Cells were also transfected with WT Myc-Rab35 for the last 48 h of the siRNA treatment, harvested, lysed, separated by SDS-PAGE and immunoblotted with anti-Myc and anti-actin antibodies. (C-E) Cells on cover-slips were fixed and immunostained with anti-MICAL-L1 antibody followed by 568-conjugated anti-mouse antibody. (E) Quantification of (C) and (D). One hundred cells of each treatment from three independent experiments were analyzed to assay for MICALL1 tubular endosomes. Error bars denote standard error. Bar, 10 μm.

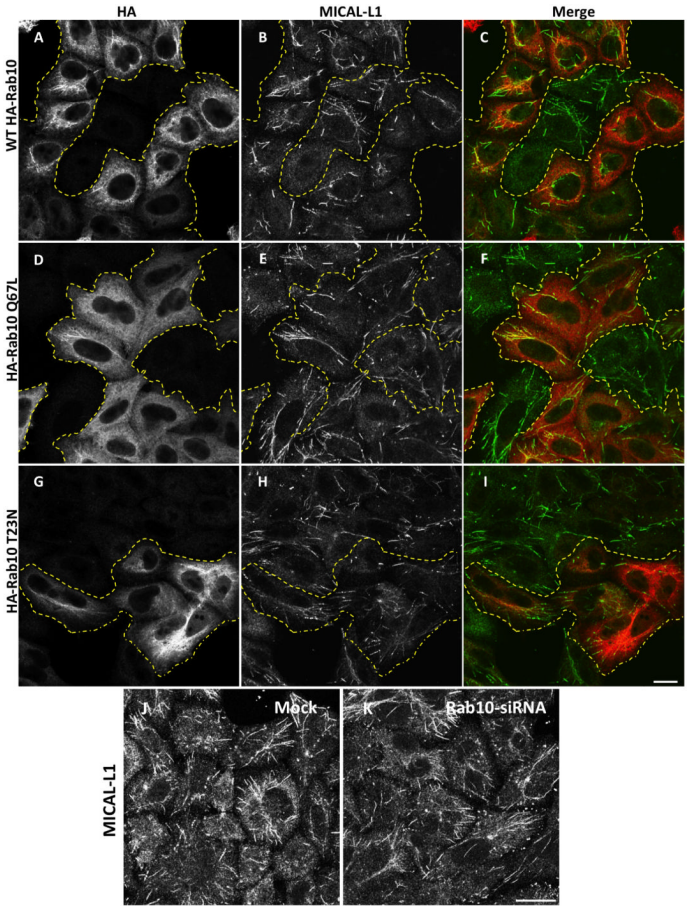

Figure 3. MICAL-L1 localization is impacted by Rab35, but not Rab10

HeLa cells were transfected with either WT HA-Rab10 (A-C), HARab10 Q67L (D-F) or HA-Rab10 T23N. After 24 h, cells were fixed and immunostained with anti-MICAL-L1 and anti-HA antibodies. Dashed borders depict transfected cells. In J and K, cells were either mock-treated (J) or treated with Rab10-siRNA (K) for 48 h. Cells were then fixed-permeabilized and immunostained with anti-MICAL-L1 antibodies. Bar, 10 μm.

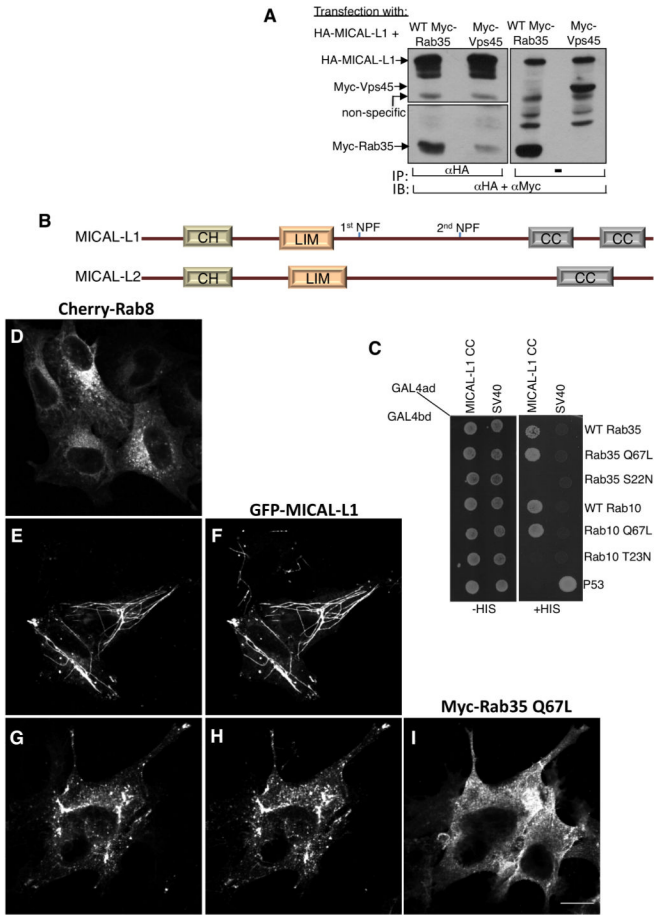

Figure 4. Rab35 co-immunoprecipitates with MICAL-L1

(A) HeLa cells were transfected with HA-MICAL-L1 and either WT Myc-Rab35 or Myc-Vps45 (control) for 24 h. Cells were harvested, lysed, and incubated with immobilized anti-HA beads for 2 h at 4°C. Immunoprecipitates were separated by SDS-PAGE and immunoblotted with either anti-HA or anti-Myc antibodies. (B) Domain architectures of MICAL-L1 and MICALL2. (C) The *S. cerevisiae* yeast strain AH109 was co-transformed with the indicated GAL4-binding domain (GAL4bd) fusion constructs and GALbdp53 (control), together with the indicated GAL4 transcription activation (GAL4ad) fusion constructs and GAL4ad-SV40 large T-antigen (control). Co-transformants were assayed for their growth on non-selective (+HIS) and selective (-HIS) media. CH = Calponin Homology domain; LIM = Lin11, Isl-1, Mec-3 domain; NPF = asparagine-proline-phenylalanine tripeptide motif; CC = coiled coil domain. (D-I) HeLa cells were transfected with either WT cherry-Rab8a only (A); WT Cherry-Rab8a and GFP-MICAL-L1 (B and C); or WT Cherry-Rab8a with GFP-MICAL-L1 and Myc-Rab35 Q67L (D-F) for 24 h. Cells were then immunostained with anti-Myc antibody. Bar, 10 μm.

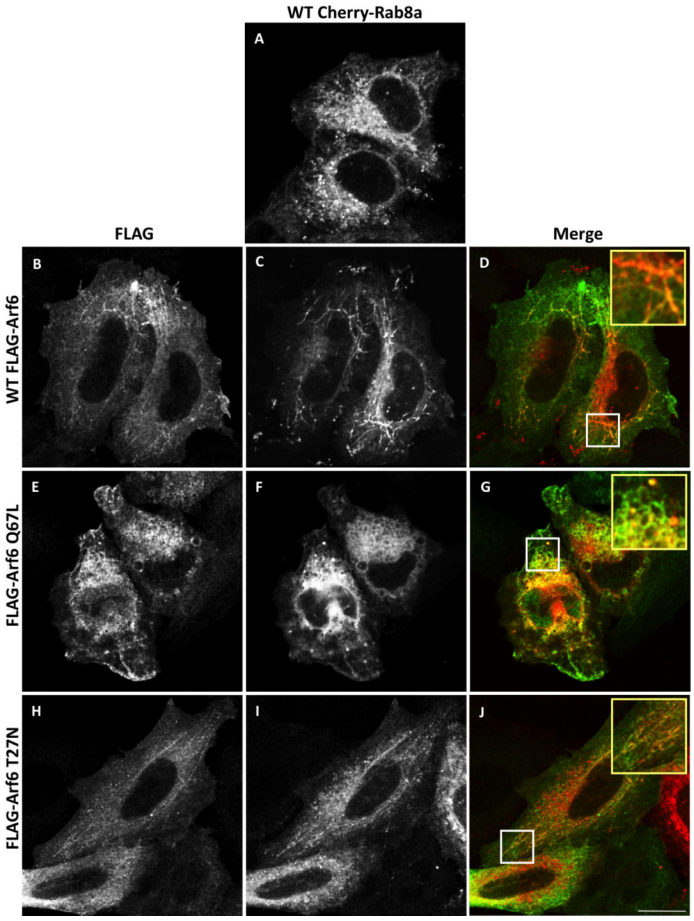

Figure 5. Arf6 controls Rab8a localization

HeLa cells were transfected with either WT cherry-Rab8a only (A); together with WT FLAG-Arf6 (B-D); together with FLAG-Arf6 Q67L (E-G); or together with FLAG-Arf6 T27N (H-J) for 24 h. Cells were fixed and immunostained with anti-Arf6 antibody. The regions within the white boxes are magnified in the yellow boxes. Bar, 10 μm.

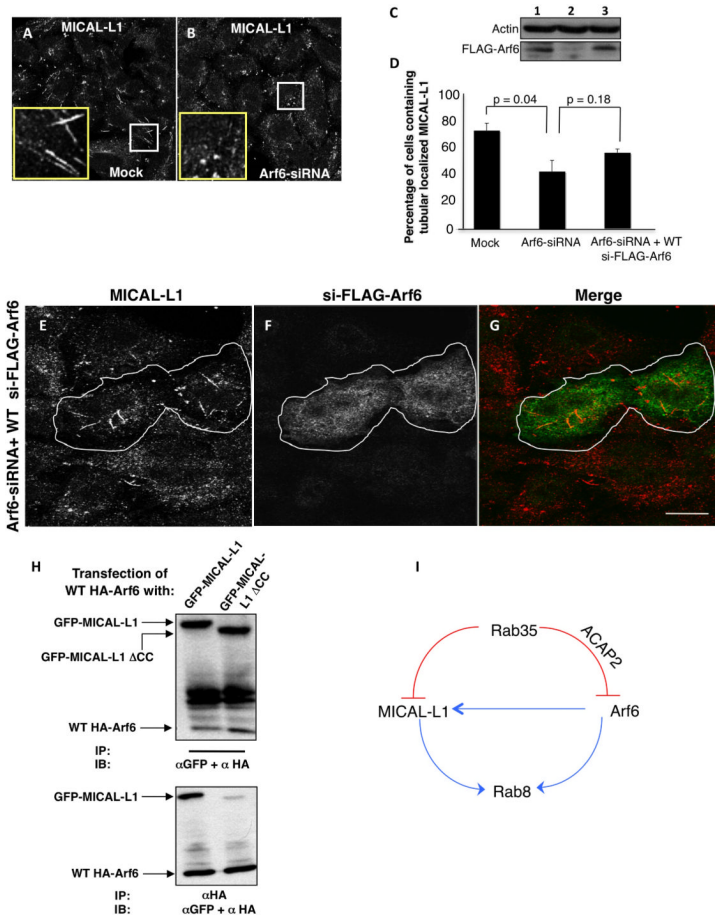

Figure 6. Arf6 interacts with MICAL-L1 and controls its recruitment to tubular endosomes

HeLa cells grown on cover-slips were either mock-treated or treated with Arf6-siRNA oligonucleotides (A and B, E-G). Some cells were also transfected with WT si-FLAG-Arf6 for the last 24 h of siRNA treatment (E-G). After 72 h of siRNA treatment, cells were fixed and immunostained with anti-MICAL-L1 and anti-FLAG antibody. (C) HeLa cells grown on 35 mm dishes were either mock-treated or treated with Arf6-siRNA oligonucleotides. Cells were transfected with WT si-FLAG-Arf6 for the last 24 h of siRNA treatment. After 72 h of siRNA treatment, cells were harvested, lysed, separated by SDS-PAGE and immunoblotted with anti-FLAG and anti-actin antibodies. (D) Quantification of E-G from three independent experiments. Regions portrayed within the white boxes are shown magnified in the yellow boxes. Bar, 10 μm. (H) HeLa cells were co-transfected with either wild-type (WT) HA-Arf6 and GFPMICAL-L1, or GFP-MICAL-L1 lacking its membrane-binding coiled coil region (GFPMICAL-L1 ΔCC). After 24 h, cells were lysed and subjected to immunoblot analysis (top panel) or co-immunoprecipitation analysis (bottom panel). (H; top panel) Immunoblot analysis depicts relatively equal expression levels of GFP-MICAL and GFP-MICAL-L1 ΔCC, as well as WT HAArf6. (H; bottom panel) Immunoprecipitation of WT HA-Arf6 was done with anti-HA antibodies. As shown, GFP-MICAL-L1 was detected in a complex with Arf6, whereas the MICAL-L1 ΔCC mutant (control) was absent. (I) Model depicting Rab35 regulating tubular localization of MICALL1 and Rab8a. Over-expression of Rab35 disrupts MICAL-L1 localization to tubular membranes, which leads to dissociation of Rab8a from the tubules. Rab35, inhibits Arf6 *via* ACAP2 activity, decreasing MICAL-L1 localization to tubular membranes. Arf6 activity is also required for Rab8a localization to tubular membranes.